MANUFACTURING AND TESTING OF THE FIRST FOUR SUPERCONDUCTING Nb CAVITIES FOR LEP

D. Bloess, G. Cavallari, E. Chiaveri, I. Gorin(*), R. Stierlin, J. Tückmantel and W. Weingarten

CERN, Geneva, Switzerland

ABSTRACT

An approach towards industrial fabrication of superconducting Nb cavities for LEP was undertaken and the experience is described. Out of the first four Nb superconducting cavities to be installed in LEP two cryostats and cavities were produced by CERN and two more by industry. The results are essentially the same. The accelerating field and Q-value at the design value are between 5.3 and 9 MV/m and between 2.0 and 3.3×10^9, respectively. The static cryostat losses were 16 W. The ancillary equipment (couplers, tuners) was produced by CERN. All the fabrication sequence applied at CERN has been used in an identical way by industry.

Presented to the 4th Workshop on RF Superconductivity
August 14-18, 1989, Tsukuba, Japan

(*) Visitor from IHEP, Serpukhov, USSR.

1. INTRODUCTION

During the last four years experience on the design of the 4 cell 352 MHz Nb LEP type cavity has been finalized such that the production of the first four cavities for LEP be launched. In a first step it was shown that the cavity proper (fig. 1) (called LEP0) could be operated according to specifications [1]. Further on, the cryostat design (fig. 2) was tested [2] and cryogenic hazards were simulated (LEP1, [3]). In a final step, a fully equipped cavity (LEP2) was installed in one of CERN's accelerators (SPS, fig. 3) to accumulate operating experience and to boost the beams of e^+e^- injected into LEP [4,5].

The positive outcome of these tests opened the way to start collaboration with industry for the production of the first four cavities (LEP3, 4, 5, 6) to be installed in LEP during a first shut down in fall of 1989, after the LEP collider has been fully commissioned.

Out of this batch of four cavities, LEP3 and LEP4, together with the cryostats, were ordered at industry (Interatom, Bergisch-Gladbach, West-Germany), the cavities LEP5 and LEP6 and their cryostats were produced at CERN. RF power couplers (fig. 4), Higher Order Mode (HOM) couplers (fig. 5) and frequency tuners (fig. 6) for these four cavities were all fabricated at CERN (table 1). In this report, we will give our experience during fabrication and test. Emphasis is put not so much on superconducting RF cavities brought to high performance by repeated repair and retreatment cycles of individual cavities, but more on industrial production methods, which are adequate to obtain the design values right away in the first test, and in the scatter of results.

TABLE 1: Manufacturer of LEP cavities and Nb sheet

	LEP3	LEP4	LEP5	LEP6
Manufacturer cavity	Interatom	Interatom	CERN	CERN
Manufacturer Nb-sheet	Hereaus	WahChang	Kawecki	Kawecki
RRR	180	150	110-230	110-160
Manufacturer cryostat	Interatom	Interatom	CERN	CERN
Manufacturer RF power couplers, HOM couplers, tuners	CERN	CERN	CERN	CERN
E_a^{max} [MV/m]	5.4	8.6	9.0	5.5

2. CAVITY PRODUCTION

The sequence of cavity production, which has finally emerged after numerous tests, is shown in table 2. The cryostat [2], RF power and HOM coupler [6], frequency tuner [7], and details and experience gained at a pilot series production at CERN [8] are described in the references quoted.

TABLE 2: Cavity production

Cavity cells	Beam tubes
Cutting 3 mm thick Nb sheet to disks (Ø 890 mm) with central hole	Rolling and shaping of tubes from Nb sheet
Extrusion of cavity iris	Brazing of Conflat flanges to beam, coupler and antenna probe tubes
Rust test in 1 °/∘∘ HCl-water	Machining of lips for He tank welds
Mechanical removal of inclusions (if necessary)	
Spinning of half cells	
Machining of welding planes	
Anodization of half cells for visual check	
Chemical Polishing (CP) by 70 μm of inner surface in $H_3PO_4/HF/HNO_3$ solution (1:1:1 by volume)	
EB-welding at equator (gun inside cell)	
Frequency check of monocells	
EB-welding at irisis (gun inside cavity)	
Leak test of cavity welds	
Measurement of field profile and frequency	
Welding of He tank and pressure test	
CP by 20 μm of inner surface (2:1:1 by volume)	
1st rinsing with demineralized water (5000 ℓ, $\rho \geq 10$ MΩcm)	
Mounting of HOM couplers	
2nd rinsing with ultrapure water (550 ℓ, $\rho \geq 18$ MΩ cm)	
Drying by pumping	
Assembly in horizontal cryostat	
RF test	

As essential points for the production and treatment we consider:

- Careful inspection of metal sheet and of cavity half shell surface and removal of inclusions (if necessary).
- EB welding with gun inside cells with protection of welding planes against contamination by dust.
- Final rinsing with large quantities of pure and dustfree water under continuous control of its resistivity [9] and rapid drying by pumping (table 3).

TABLE 3: Conditions of final rinsing with water

	LEP3	LEP4	LEP5	LEP6
Demineralized H_2O [10 MΩ cm]				
Volume [m^3]	8	8	8	8
Resistivity out [MΩcm]	9.2	7.5	6.7	6.7
Pure dust free H_2O [18 MΩ cm]				
Volume [m^3]	0.5	0.5	0.5	1.5
Resistivity [MΩcm] in	17.8	17.7	17.9	18.3
Resistivity out	9.1	8.9	6.3	5.2

The tolerance requirements to the Nb sheets or half cells allow a margin of grain size ASTM 5 to 6, thickness $\leq \pm$ 0.2 mm, ellipticity before welding $\leq \pm$ 0.6 mm. The field flatness resulting from these tolerances and the production process chosen is $\Delta E/E \leq \pm 12\%$.

The RRR of the Nb sheet material used, supplied by three different manufacturers, varied between 110 and 230 (table 1).

3. EXPERIMENTAL RESULTS

3.1 RF setup

In a first test LEP3 and LEP4 being not yet equipped with the power and HOM coupler and tuners, the RF measurement was performed with a high

Q_{ex} antenna. LEP5 and LEP6 were fully equipped cavities. LEP3 and LEP4 were tested with 200 W RF power, and a 5 kW tetrode amplifier, if necessary. For LEP5 and LEP6 the RF power was supplied by a Thomson 60 kW tetrode, connected to the cavity by a flexible coaxial RF cable (fig. 7). In a later test LEP3 and LEP4 were also fully equipped and tested with the 60 kW tetrode.

The high power RF setup resembles very much the one chosen for the test in the SPS [4, 10]. It is in so far unconventional as no circulator is used. On a 50 Ohm load, the tetrode can supply 60 kW forward power. In that case the reflected wave vanishes. However, for the superconducting cavity without beam load, the reflected wave has nearly the same amplitude as the incident wave. This limited the RF voltage being composed of the sum of the incident and reflected wave. Thus the tetrode supplies in this case only up to 1/4 of the maximum power (15 kW). This is not sufficient to obtain an accelerating field E_a = 5 MV/m, as according to the $Q_{ex} = 2 \times 10^6$ a forward power of 20 kW is needed. That is why a transformer element (fig. 8) is installed in the coaxial part of the RF feeding line, which has a transformer ratio n = 70 Ω/35.7 Ω = 2(≃ 5.8 dB), such that the maximum incident power in the power coupler is 60 kW, which is largely sufficient. Its design was optimized by means of a computer code to compensate for stray capacities [11].

The experimental results are summarized in the tables 4 to 7.

3.2 RF results

In table 4 the RF results at 4.4 K, the operating temperature, and in fig. 9 the Q-value versus the accelerating field E_a is shown.

The cavity and the cryostat were protected by two kinds of interlocks, which, when activated, cut the RF power [12]. A fast interlock was tripped, whenever the pressure of the liquid He bath, the pressure of the cavity or the γ-radiation were too high. A slow interlock was tripped, whenever during the intermittent readout by computer (every 4 seconds) a temperature (RF window, tuner bar, tuner exciting coils, power coupler) or the liquid He level were out of the tolerable range.

TABLE 4: RF performance at 4.4 K

	LEP3	LEP4	LEP5	LEP6
E_a^{max} [MV/m]	5.4	8.6	9.0	5.5
Field limitation	Q	RF	Q	Q
Q (E_a → 0 MV/m) [10^9]	3.0	2.7	–	–
Q @ 5 MV/m [10^9]	2.2 ± 0.3	2.2 ± 0.3	3.3 ± 0.7 [a]	2.0 ± 0.7 [a]
Processing time [h]	1	1	3.5	8
γ [m Sv/h]	5	3	1.3	> 10
Vacuum at start of cooldown [10^{-7} mbar]	1	2.1	0.3	0.4

Legend:
- E_a^{max} = maximum accelerating field
- Q = fast thermal breakdown ("quench")
- RF = Max. tolerable RF power
- Processing time = time of RF processing to obtain 5 MV/m
- γ = γ-radiation at end of test @ 5 MV/m
- (a) = Cryogenic measurement of RF losses

3.3 Results on tuners and couplers

The dynamic frequency tuning of the cacity is accomplished by three bars made of nickel which form the supporting frame of the cavity [7]. Their length determines the overall length of the cavity and hence its frequency. It is controlled by varying the temperature (slow thermal tuner) and by exciting a magnetic field (fast magnetostrictive tuner).

In absence of RF signals the average temperature of the thermal tuner is controlled to keep the variation of the resonance frequency of the cavity within the range of the magnetostrictive tuner. The He gas mass flow passing the tuner bars has to remain constant within ± 10%.

The measured performance is listed in table 5. In addition we have measured the dependence of the resonant frequency of the cavity on the He bath pressure (3 Hz/mbar) and resonant frequencies of acoustic modes of the cavity (44.0, 59.6, 93.2, 98.4 Hz). The most favourable operating temperature of the tuner is around 150 K, the central point of the temperature setting interval. For the tuner bars at 4.5 K the nominal LEP frequency of 352.209 MHz corresponds then to 352.184 MHz. Under these conditions the resonant frequency of the cavity, measured after the first cooldown, scattered around this value by $\{^{+\,202}_{-\,8}\}$ kHz. Therefore, in general, the overall length of the cavity has to be readjusted before the final assembly of the cavity into modules of four.

In cooling down the cryostat the resonant frequency of the cavity is increased by 460 kHz.

<u>TABLE 5</u>: Tuner performance

	LEP3	LEP4	LEP5	LEP6
Range [kHz] of thermal tuner (4.4 ÷ 300 K)	51	50	55	57
Range [kHz] of magnetostrictive tuner (0 ÷ 5 A)	1.9	2.0	1.5	1.5
Resonant frequency of cavity (first cool down, tuner bars at 4.5 K)[MHz]	352.386	352.186	352.239	352.176

The performance of the power coupler and HOM couplers are listed in tables 6 and 7.

The HOM coupler is cooled by a channel connecting it to the liquid He bath. It was observed that sufficient cooling was extremely important for a correct functioning. Otherwise, the HOM coupler heated up and changed its Q_{ext}, such that up to 100 W RF power in the fundamental mode were coupled to the RF load at room temperature.

TABLE 6: External Q-values of fundamental mode

	LEP3	LEP4	LEP5	LEP6
Power couplers [10^6]	1.6	1.4	1.8	2.0
RF probe [10^{11}]	0.9	0.9	1.6	1
HOM coupler @ 352 MHz [10^{10}]	4.0/3.8	32/240	61/21	22/26

The external Q-values of the HOM were damped down to some 10^4 (table 7).

TABLE 7: External Q-values of some HOMS (LEP3)

Mode	Frequency [MHz]	Q_{ext} [10^4]
TE	462.24	1.0
TE	462.54	2.1
TE	477.14	0.9
TE	477.40	2.2
TM_{110}	507.46	2.2
TM_{110}	507.58	5.0
TM_{110}	515.07	6.4
TM_{110}	515.15	13.9
TM_{011}	634.51	0.7
TM_{011}	637.38	1.0
TM_{111}	687.05	0.7
TM_{111}	687.29	3.8
TM_{012}	1005.55	1.9

3.4 Cryogenic measurements

The cold tests were performed at the old BOC refrigerator of CERN, which delivers up to 450 W refrigeration power at 4.5 K. Flexible transfer lines connected the cold box and the cryostat.

After every RF test the cryostat static losses were determined by measuring the evaporation rate, corresponding to less than 16 W heat input into the liquid He. Three independent He gas mass flows of 4.4 K are used, one (0.1 g/s) to cool the beam tubes, radiation shields, tuner exciting coils and inner conductor of the power coupler, one (0.1 g/s) for the three Ni bars of the thermal tuner, and one (0.01 g/s) to intercept the heat conducted along the outer wall of the power coupler. To avoid oscillations of the cryogenic system, in particular of the liquid He pressure and level in the cryostat, it was necessary to maintain the sum of static heat load and RF heat load constant by an electrical heater in the liquid He bath of the cryostat. The latter controls the liquid He pressure in the cryostat to ± 5 mbar. In addition it gives at hand the possibility to determine the Q-value by the increase of heater power if the RF is switched off. The liquid He level is controlled by the liquid He supply valve of the refrigerator to ± 1 ℓ (± 10 mm).

3.5 Results on the assembly of components

The two cavities produced by industry being tested, the HOM and RF power couplers were mounted. When the coupler ports are open, a steady flow of filtered nitrogen gas prevents dust particles to enter. LEP3 was retested and essentially the same RF results were found as before. The γ-activity (~ 5 m Sv/h) has also remained unchanged. With LEP4, however, we experienced a decrease of the maximum accelerating field to 3 MV/m, caused by a quench. From the variation of the maximum field (measured by an RF probe in one of the beam tubes) for the four different passband modes with unflat cell excitation it was concluded, that a defect in one of the end-cells limited the field. This was confirmed by inspection by eye, which revealed a black spot there. The cavity was retreated (CP of 20 μm) and retested, the maximum field was 7.1 MV/m, limited by a quench. Apart from this cavity, the three other ones are already assembled together into one module (fig. 10), which will finally consist of four individual cavities [13].

4. DISCUSSION

The accelerating field obtained surpassed the target value of 5 MV/m for all four cavities, the maximum value being at 9 MV/m. The improved and longer rinsing with ultrapure water seems to be the reason why the maximum field was obtained after some hours only of high field operation without admitting He has into the cavity ("He-processing"). The field limitation was either the maximum power rating in vacuum of the type N connector (200 W c.w., LEP4), or induced by a fast thermal quench. The electron loading was small enough not to affect the Q-value up to the maximum field.

However, the Q-value at 5 MV/m is lower than the design value. To find out the reason one cavity (LEP4) was cooled down under different static magnetic field configurations. The magnetic field at the cavity surface $\vec{H}_{ext}$ is the sum of the ambient field $\vec{H}_o$ and the field generated by the arrangement of coils $\vec{H}_c$: $\vec{H}_{ext} = \vec{H}_o + \vec{H}_c$. The cryostat was cooled down for $\vec{H}_c = -\vec{H}_o$, 0, $\vec{H}_o/2$ and $\vec{H}_o$, corresponding to H_{ext}/H_o = 0, 1, 1.5 and 2. From the low-field Q-value, knowing the BCS Q-values, the residual Q-value Q_{res} was determined (fig. 11). The straight line shows the residual losses ($1/Q_{res}$) vs. the external magnetic field H_{ext} in units of the ambient magnetic field H_o (490 mG). For an ideal magnetic field compensation ($H_o \rightarrow 0$ mG) the residual losses would correspond to a Q-value of 2×10^{10}. The measured residual losses ($Q_{res} = 6.6 \times 10^9$) correspond to a residual average magnetic field $H_{ext}/H_o = 30\% \hat{=} 150$ mG at the surface of the cavity. However, computer calculations for the magnetic field compensation actually used and for a homogeneous ambient magnetic field showed that the absolute value of the resulting magnetic field at the cavity surface should be $H_{ext}/H_o = 12\% \hat{=} 60$ mG. We conclude, therefore, that field inhomogeneities cause residual losses higher than expected. This observation among others [5] led us to abandon the method of magnetic field compensation by coils and to use high permeability magnetic shielding instead.

We experienced that the vacuum at the start of the cooldown should be lower than 1×10^{-7} mbar in order to avoid strong e^- loading at accelerating fields below 5 MV/m.

5. CONCLUSION

All 4 cavities surpassed the design value of accelerating field (5 MV/m) in the first test, one cavity even went up to 9 MV/m. The field limitation was either the admissible RF power or a thermal quench. The prolonged water rinsing (compared to our previous practice) made it possible to obtain the maximum field within some hours of operation without He-processing. The Q-value at 5 MV/m was between 2 and 3.3×10^9, being limited by magnetic field inhomogeneities. In one case, after assembly of the power and HOM couplers, a cavity degraded and had to be recovered by CP.

Acknowledgements

We would like to thank all technicians involved in the work described, those of the RF and cryogenics groups of EF Division, and those of CERN's central workshops, for their untiring effort. We appreciated the fruitful collaboration with Interatom Company, in particular with H.P. Vogel. Ph. Bernard and H. Lengeler contributed with competent advice and steady encouragement.

REFERENCES

[1] G. Arnolds-Mayer et al., IEEE Trans. Nucl. Sci. NS-32 (1985) 3587.

[2] R. Stierlin, Proc. 3rd Workshop RF Superconductivity, Argonne, Ill., USA, ANL-PHY-88-1, Ed. K.W. Shepard, 639.

[3] G. Cavallari et al., this Workshop.

[4] Ph. Bernard et al., Proc. EPAC, 7-11 June 1988, Rome, Italy (1988) 988.

[5] D. Boussard et al., Proc. Part. Acc. Conf. 1989, Chicago, Ill., USA, to be published in IEEE Trans. Nucl. Sci..

[6] G. Cavallari, ibid. ref. 2, 565.

[7] G. Cavallari, ibid. ref. 2, 625.

[8] E. Chiaveri, CERN/EF/RF 89-7.

[9] Y. Kojima and K. Saito, private communication.

[10] D. Boussard et al., ibid. ref. 4, 985.

[11] H.P. Kindermann, private communication.

[12] G. Cavallari and E. Ciapala, LEP RF Note 22 (CERN/EF/RF 88-4).

[13] C. Arnaud et al., this Workshop.

FIGURE CAPTIONS

Fig. 1 Four-cell LEP prototype cavity produced from Nb sheet metal during assembly of the helium tank around the cavity.

Fig. 2 LEP prototype cryostat with stainless steel vacuum jacket removed for access to cavity.

Fig. 3 LEP prototype cavity in SPS tunnel.

Fig. 4 RF power coupler.

Fig. 5 Higher order mode coupler.

Fig. 6 Frequency tuner bars with heater (in the middle) and coils (at the right and left half of the bar).

Fig. 7 Test layout with tetrode and flexible coaxial RF cable (left) phase shifter and cryostat (right).

Fig. 8 Coaxial line RF transformer with transformer ratio 2.

Fig. 9 $Q(E_a)$-curve for cavity LEP4.

Fig. 10 Cryogenic module housing four cavities in the final version. On the photo, already three cavities are assembled together in one cryostat.

Fig. 11 Inverse residual Q-value vs. external static magnetic field H_{ext} (measured in units of the ambient field H_o = 490 mG), generated by arrangement of coils.

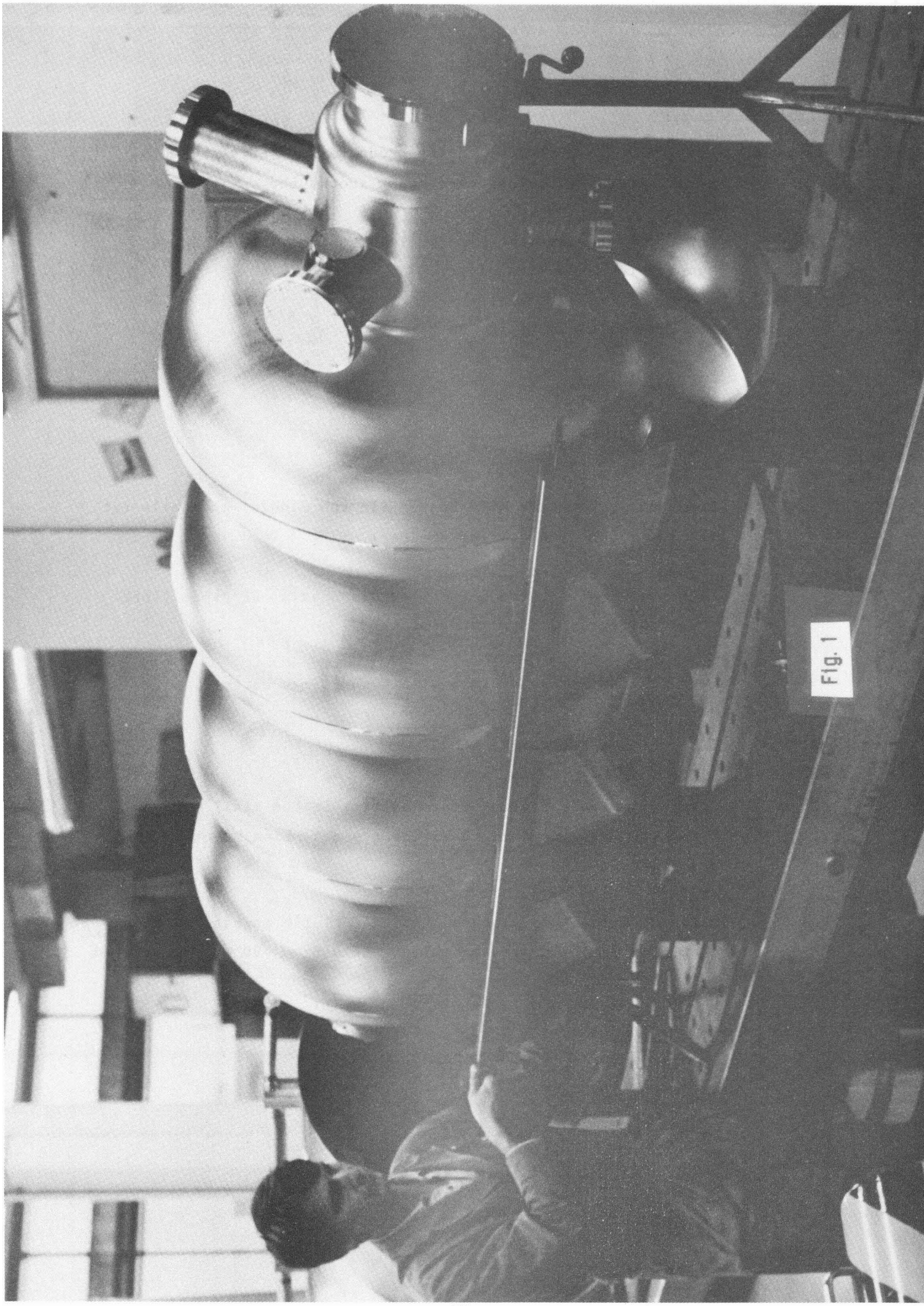

Fig. 1

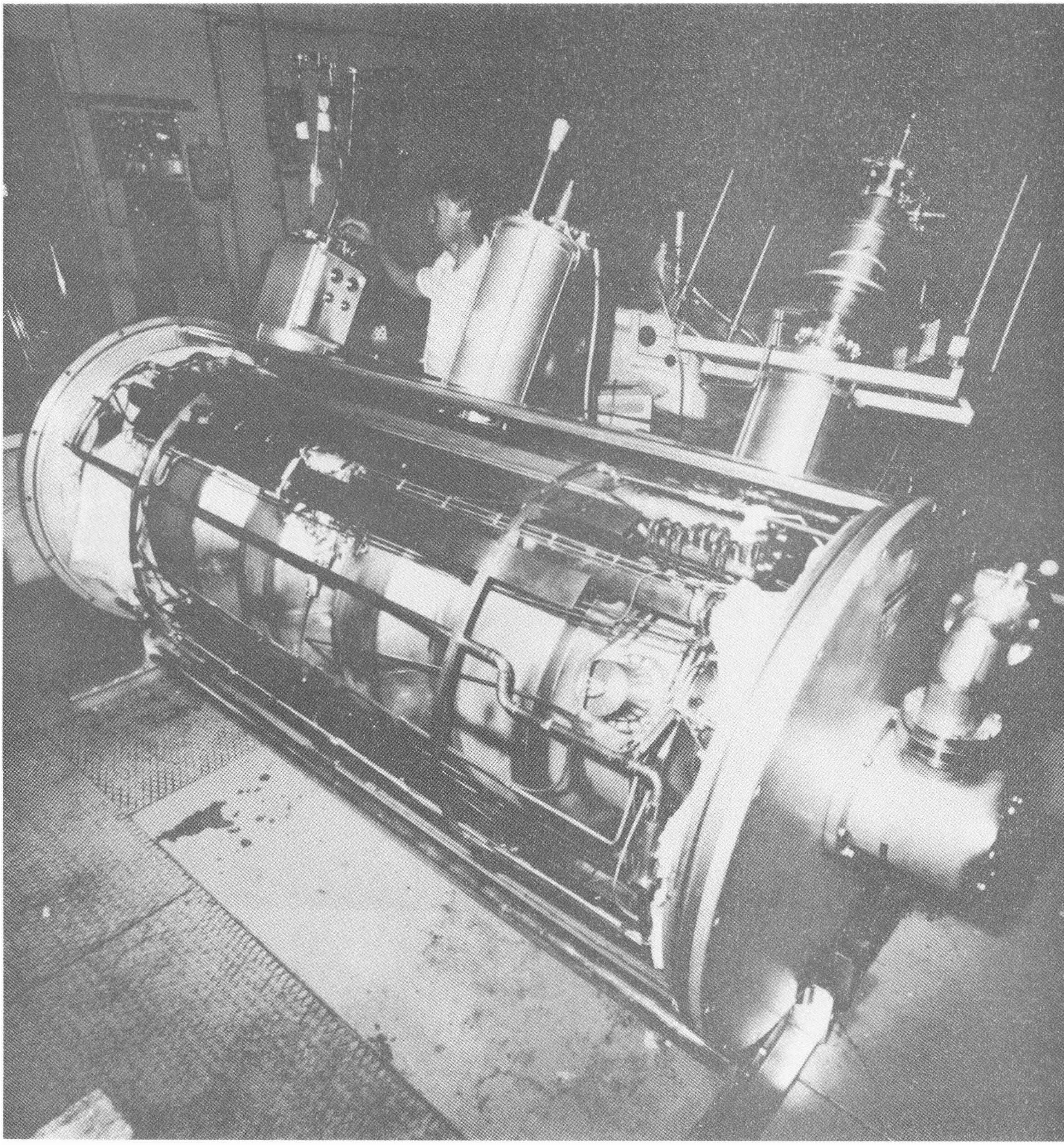

Fig. 2

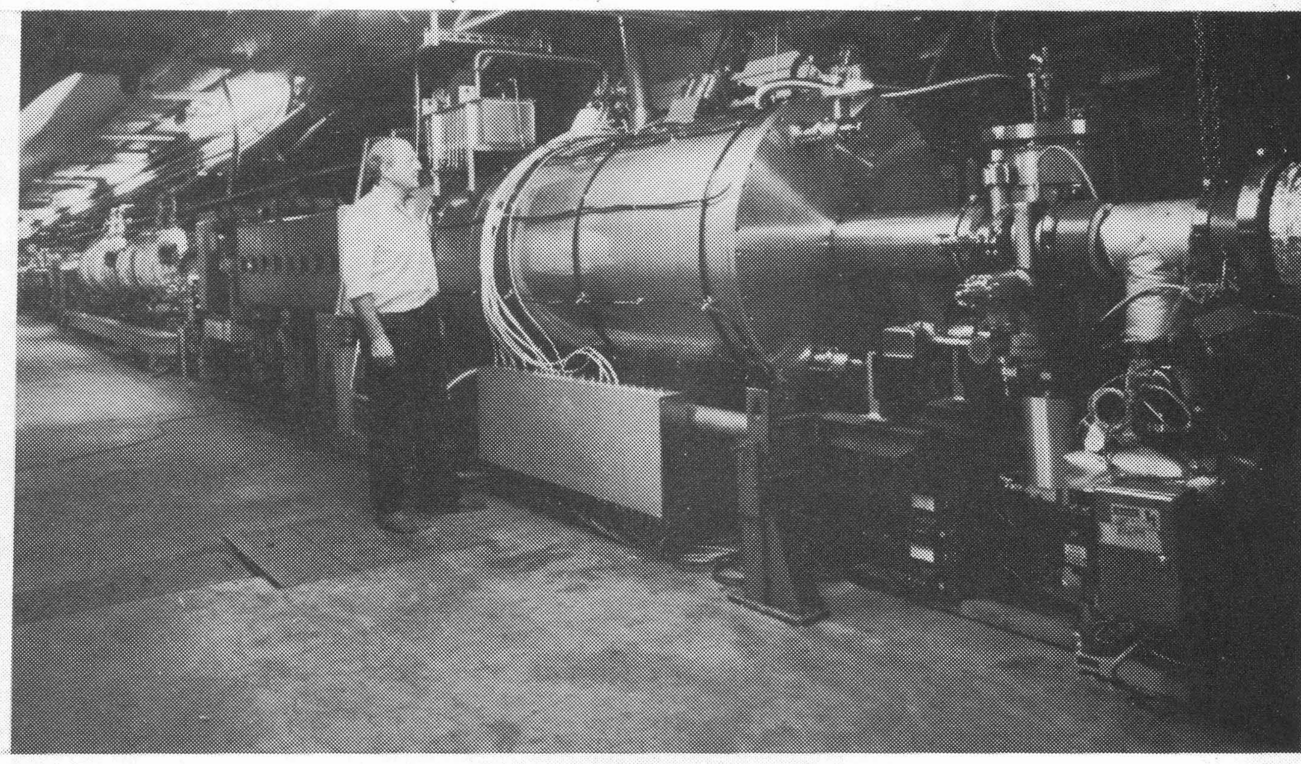

Fig. 3

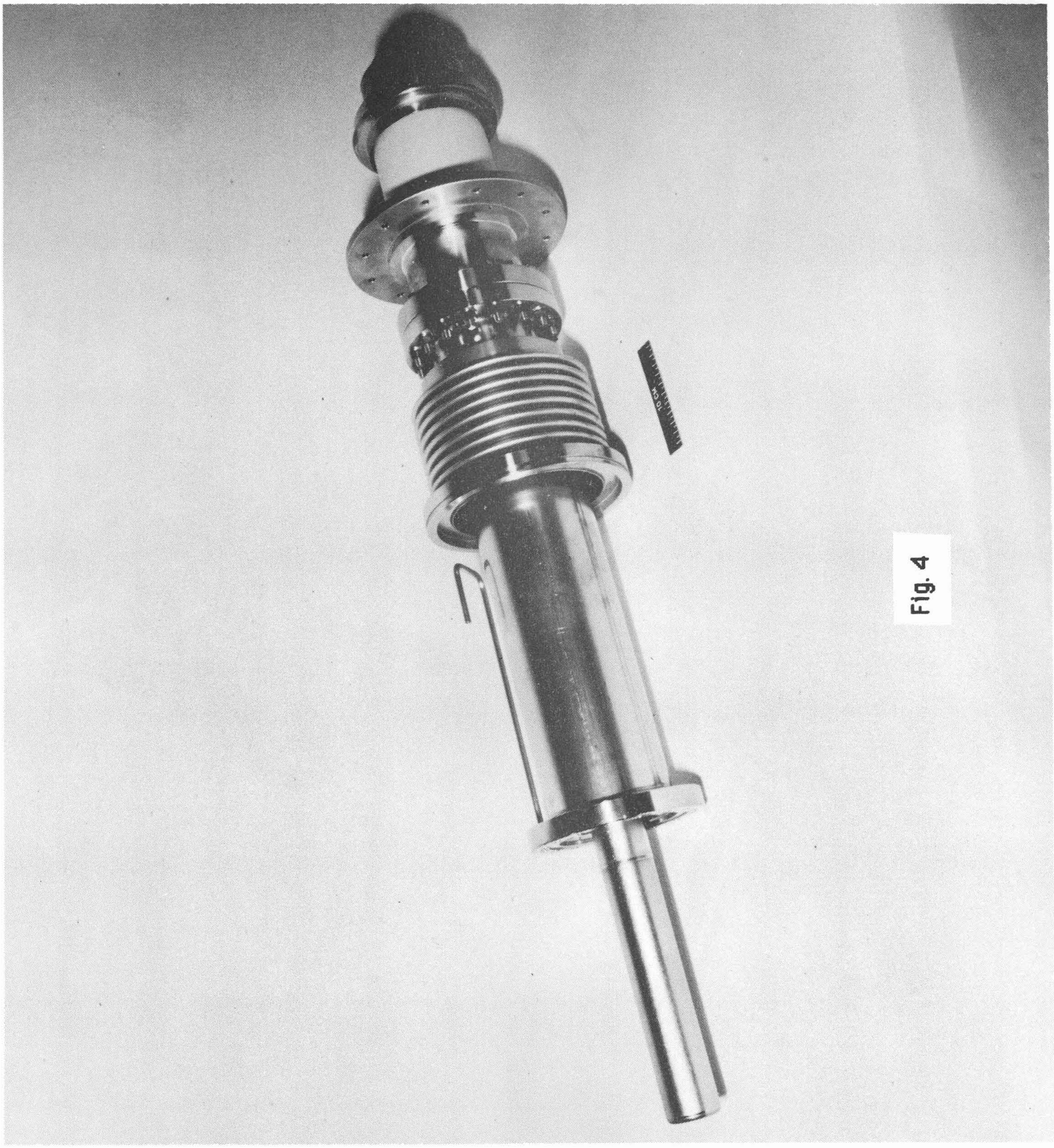

Fig. 4

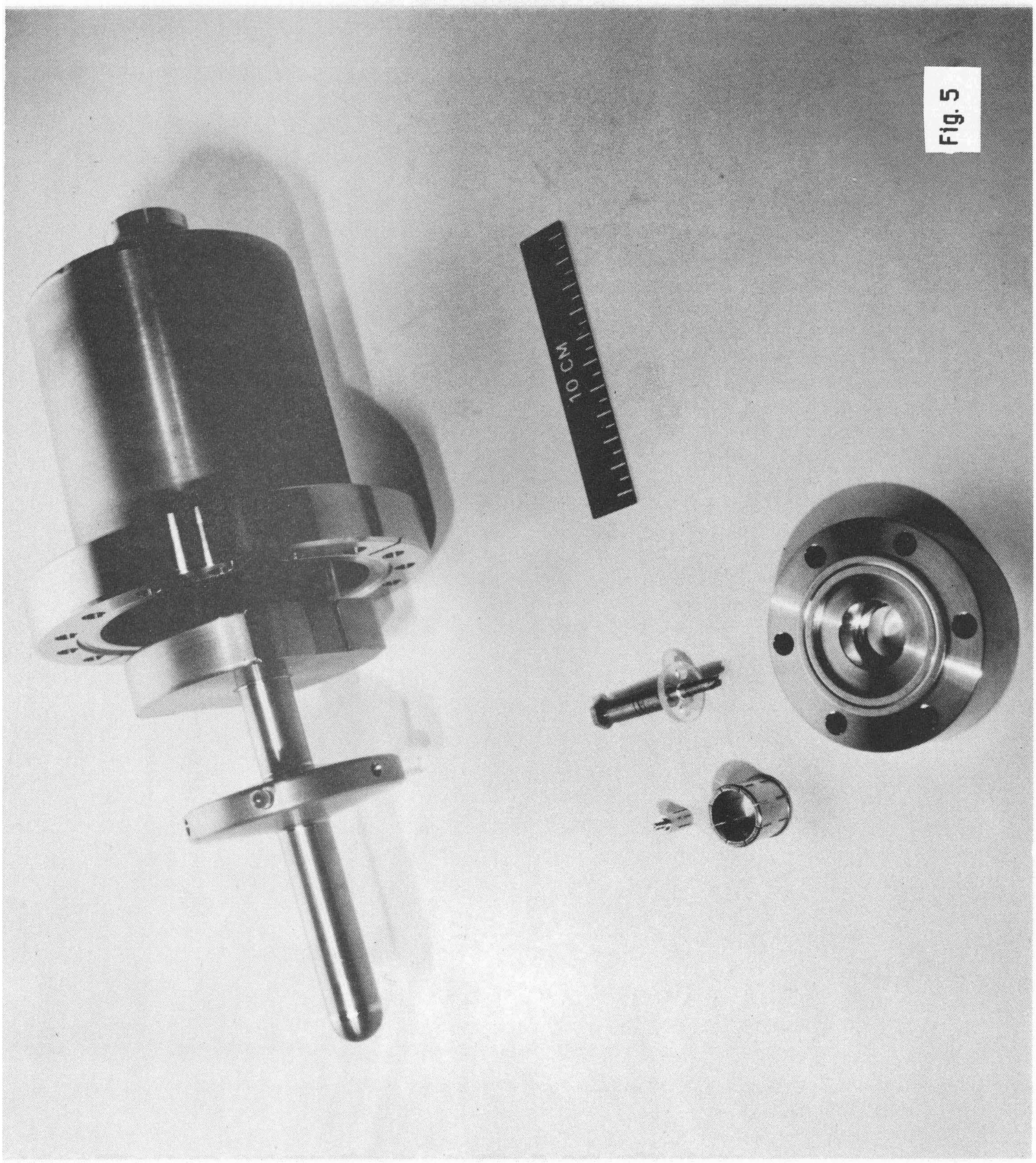

Fig. 5

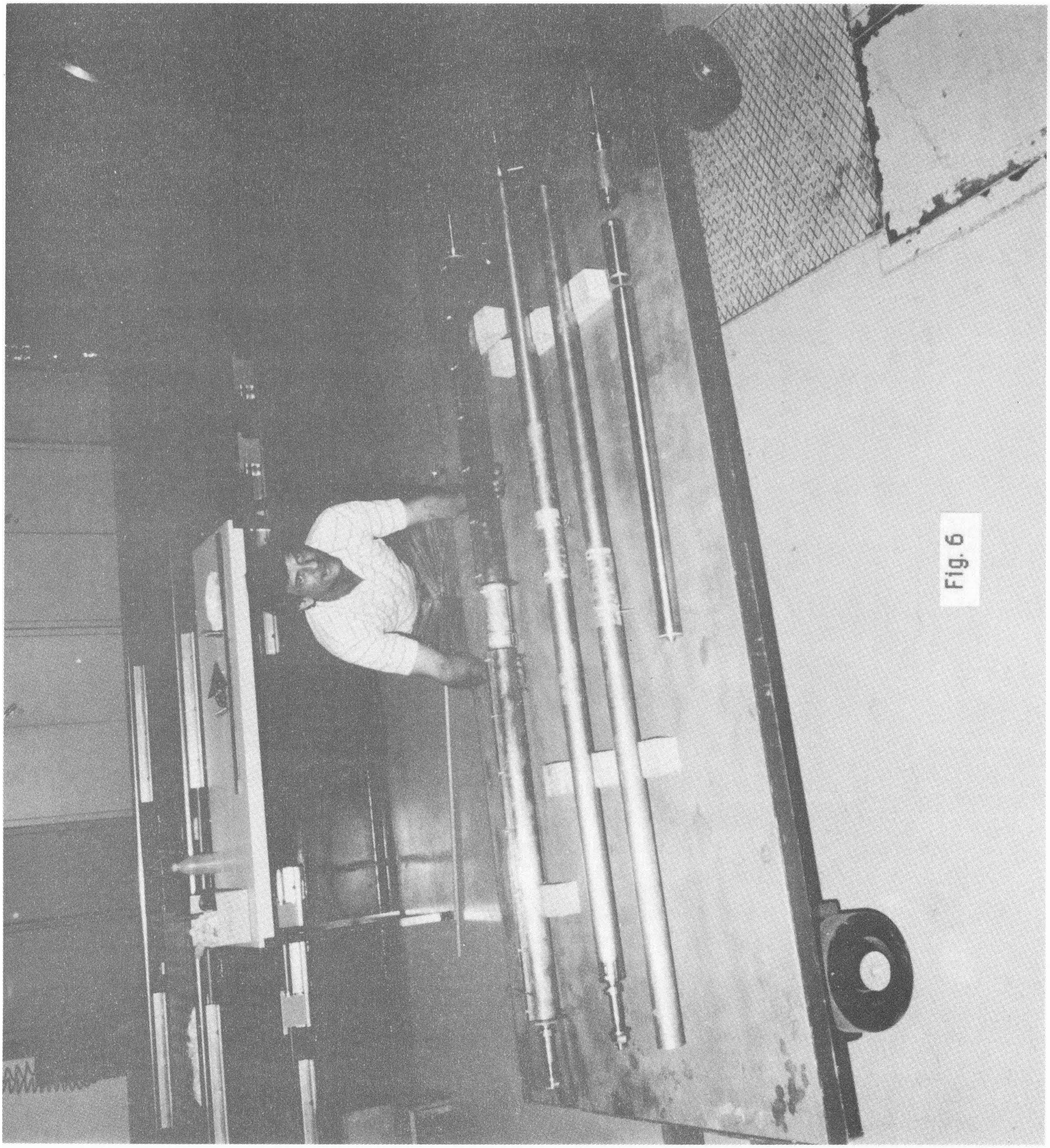

Fig. 6

Fig. 7

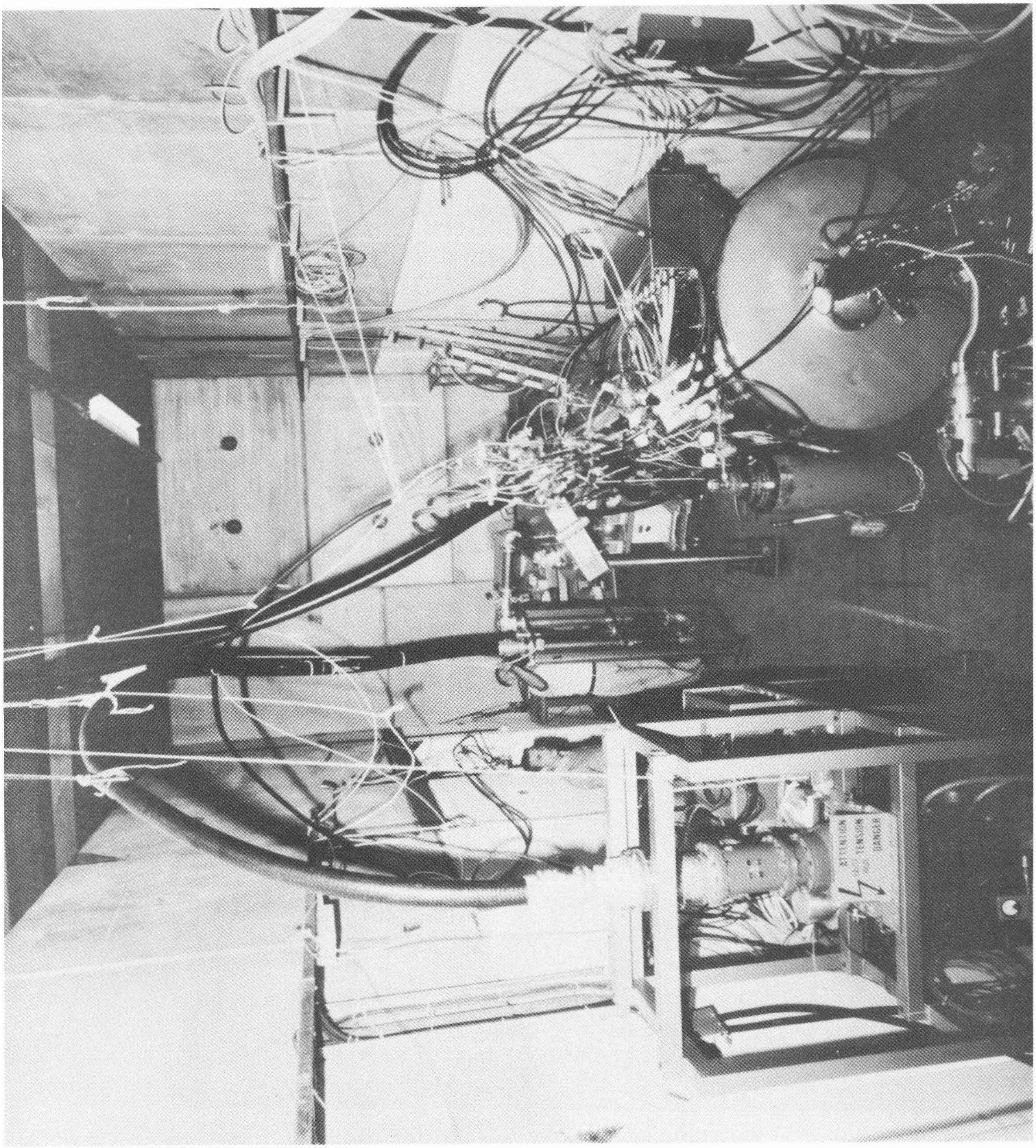

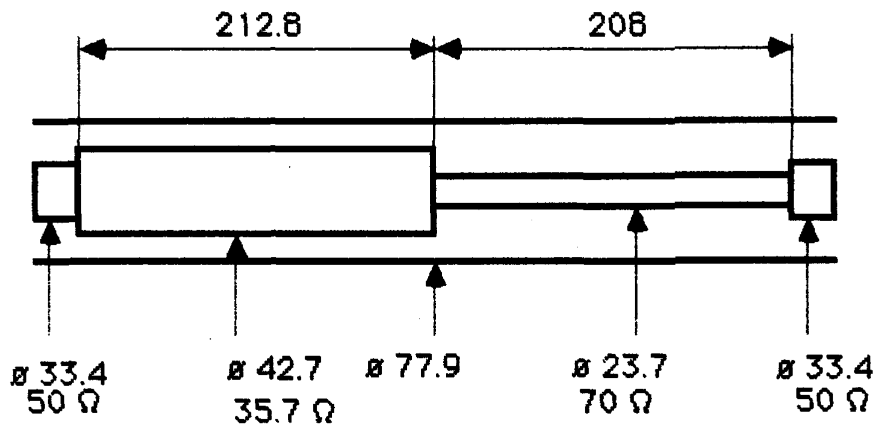
212.8
208
ø 33.4
50 Ω
ø 42.7
35.7 Ω
ø 77.9
ø 23.7
70 Ω
ø 33.4
50 Ω

Fig. 8

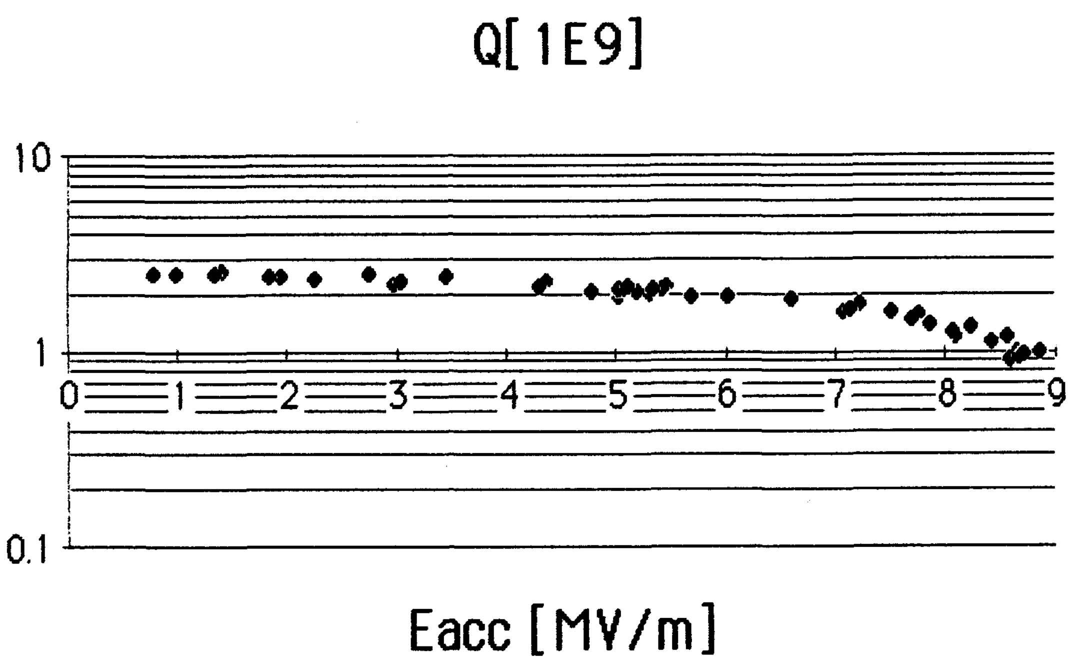
Q[1E9]
10
1
0.1
0
1
2
3
4
5
6
7
8
9
Eacc [MV/m]

Fig. 9

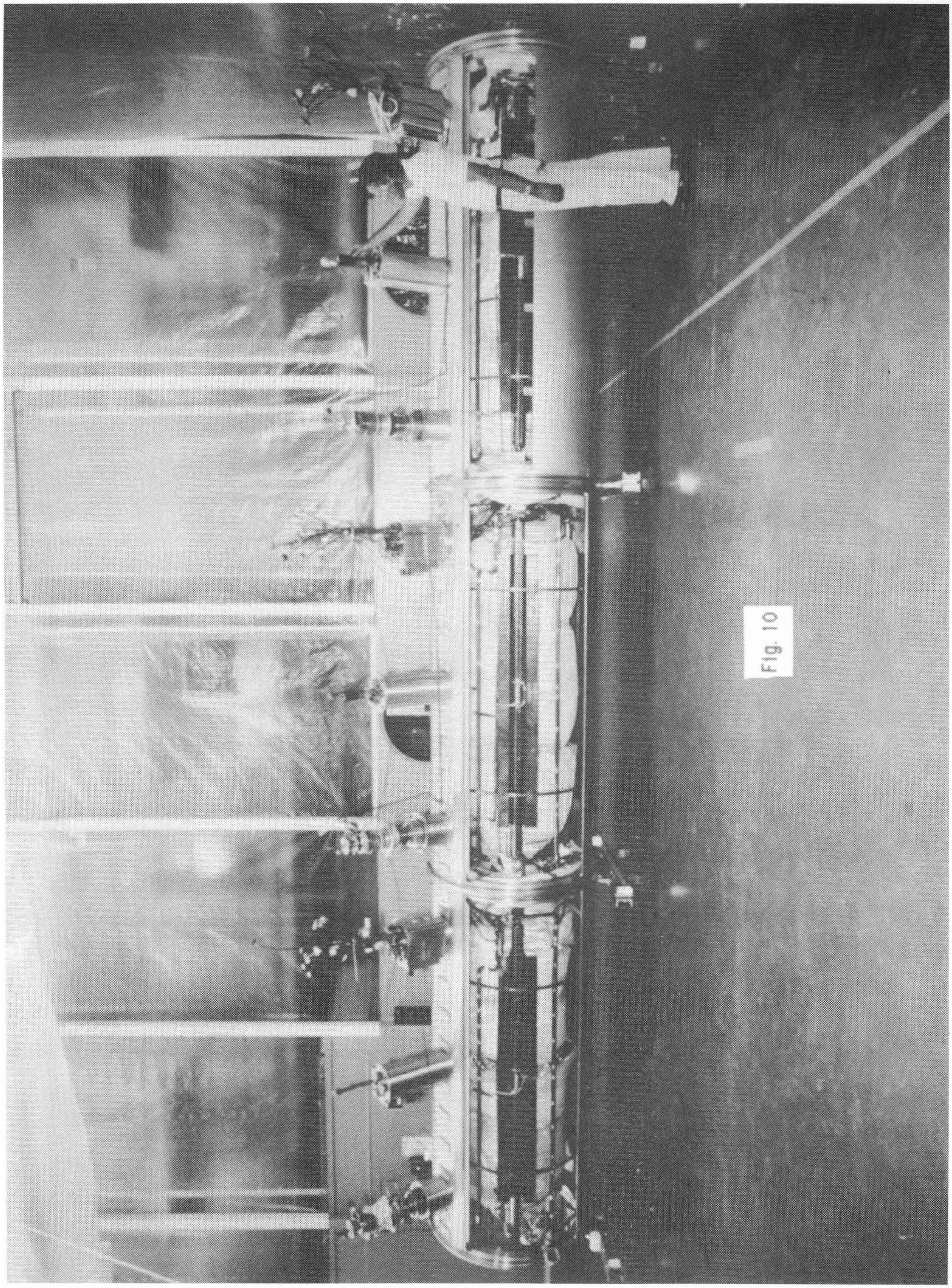

Fig. 10

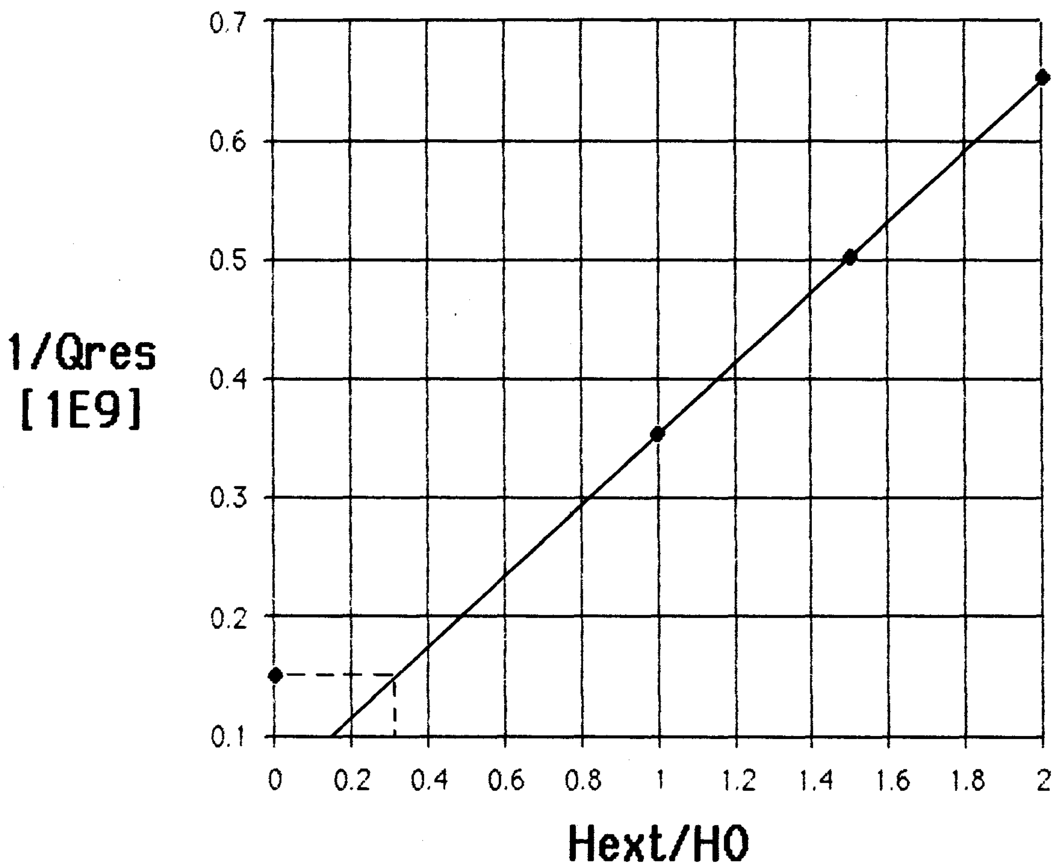

Fig. 11